2023 IEEE IAS Global Conference on Renewable Energy and Hydrogen Technologies (GlobConHT)
The Maldives National University, Male City (Maldives). Mar 11-12, 2023

Operational Risk for Integrated Power and Gas Systems Considering Varying Hydrogen Concentrations With High Penetration of Wind

Sheng Wang
State Key Laboratory of Internet of Things for Smart City,
Department of Electrical and Computer Engineering
University of Macau
Macao, China
shengwang@um.edu.mo

Hongxun Hui
State Key Laboratory of Internet of Things for Smart City,
Department of Electrical and Computer Engineering
University of Macau
Macao, China
hongxunhui@um.edu.mo

2023 IEEE IAS Global Conference on Renewable Energy and Hydrogen Technologies (GlobConHT) | 979-8-3503-3211-7/23/$31.00 ©2023 IEEE | DOI: 10.1109/GLOBCONHT56829.2023.10087839

***Abstract*—We establish an operational risk assessment approach for integrated power and gas systems (IPGS) considering varying hydrogen concentrations with high penetration of wind. First, the operational availability of wind generation is formulated considering the stochastic process of wind is developed. Then, an operational risk mitigation scheme (ORMS) is devised to minimize both load shedding and gas security violation. The varying gas composition on the physical properties of IPGS is characterized to fully reflect the impact of alternative gas on the IPGS operation. Moreover, several risk indices, improved from traditional gas security indices, are proposed to evaluate gas security under various uncertainties. An analytical risk evaluation method is used for better computation efficiency. Finally, a test IPGS is utilized to demonstrate the proposed approach. We can find that the proposed operational risk evaluation approach is able to evaluate the weak spot of the IPGS when distributed injections of hydrogen are considered, and the trend of the risk evolution can also be obtained during the operation.**

***Index Terms*—Operational risk, integrated power and gas systems, hydrogen, wind generation**

I. Introduction

As many countries have announced their ambitions for carbon neutralization in the energy system, the large-scale use of green hydrogen is gaining more attention recently. For example, in 2020, the UK government is planning to realize 5GW of green hydrogen capacity [1]. Green hydrogen can be produced by power-to-gas (PTG) facilities by consuming renewable energies (such as wind generation), which is also considered an effective measure to accommodate surplus renewable energies. This gives the opportunities for the development of integrated power-gas systems (IPGS), which can fully coordinate the two formal isolated power and gas systems. Besides, the injection of hydrogen can be analyzed more systematically.

This work is supported in part by the Science and Technology Development Fund, Macau SAR (File no. SKL-IOTSC(UM)-2021-2023, File no. 0003/2020/AKP), and the Natural Science Foundation of Jiangsu Province, China (BK20220261).

The hydrogen produced by PTG can be transported in different ways, such as the tube trailer, the specialized hydrogen network, or blending with natural gas (NG) in the pipelines. The last approach is a midterm and compromised solution, which is the recent focus in many countries. Because it can utilize the existing gas pipeline, the investment cost can be saved. Because the volume of hydrogen is relatively small, the hydrogen is able to sufficiently blended with the NG without extra equipment. However, the characteristics of hydrogen varies from NG in some aspects, and therefore induce risks into the existing IPGS. For example, hydrogen has a lower heat value. If the hydrogen proportion is large, the gas appliance consumes the same amount of gas and produces less heat. As a result, the gas appliance can not perform in a satisfactory way [2]. Moreover, the hydrogen has a higher flame speed. More hydrogen probably means more risks of fire hazard [3]. Because the hydrogen distribution after the injection follows the physical laws of energy flow, we need to conduct the risk of hydrogen injection in the IPGS in a systematical view.

The impact of hydrogen through PTGs has been analyzed in some previous studies. The participation of PTG is considered in the scheduling of generations with large share of renewable energies is studied in [4]. The optimal operation of PTG in active distribution system is cooptimized with the incoperation of local heat system, which is studied in [5]. The hydrogen system and electricity system is cooptimized for better providing the needs for parking lot is proposed in [6]. The comprehensive optimization-based tech-economic assessment of hybrid renewable electricity-hydrogen virtual power plants is investigated in [7]. The transportation and distributed electricity systems in city level can be cooptimized with the participation of hydrogen fueled cars, which is investigated in [8]. However, in these studies, the system operator just acts as a receiver of the hydrogen, and they do not take active measures to mitigate the negative impact of alternative gas, which makes these evaluations less practical.

Recently, there are several studies begin to concentrate on regulating the gas concentrations considering the blending of hydrogen. The IPGS considering hydrogen blending and concentration monitoring is modeled in [3]. The distributed robust hydrogen optimization in the multi-energy system with a large share of wind is developed in [9]. The distribution level IPGS coordinated with hydrogen is further investigated in [10]. The operational deasible region of various PTGs in IPGS distribution systems with hydrogen is explored in [11]. A comprehensive security modeling technique of IPGS with the participation of hydrogen is proposed in [12], and is solved using the sequential programming method. However, these researches focus on regulating the gas composition on a deterministic basis, while the operational risks considering multiple uncertainties (wind uncertainties, inherent failure, repairs, etc.) have not been evaluated yet.

Focusing on these drawbacks, this paper proposes an operational risk assessment method for IPGS considering varying hydrogen concentrations with high penetration of wind. First, a multi-state operational availability model of wind generation considering the stochastic process of wind is developed. Then, an operational risk mitigation scheme (ORMS) is devised to minimize both load shedding and gas security violation. The varying gas composition on the physical properties of IPGS is characterized to fully reflect the impact of alternative gas on the IPGS operation. Moreover, several risk indices, improved from traditional gas security indices, are proposed to evaluate gas security under various uncertainties. An analytical risk evaluation method is used for better computation efficiency. Finally, an IPGS test system is utilized to demonstrate the superiority of the proposed approach.

II. Operational Availability Models of IPGS Components

The wind farm consists of many small wind turbines, which are driven by the wind. Therefore, the electricity generations of them depends on two factors: 1) wind speed; 2) states of turbines. These two factors are stochastic and will change with time during the operation. Therefore, to deliver the operational availability model, it should be a prerequisite to characterize these two stochastic factors.

From historical data, the value of wind speed can be clustered into several infinite levels, here we call them different states, $v_i = \{v_{i,1}, ..., v_{i,h}, ..., v_{i,H}\}$. v_i represents set of wind speed on bus i; $v_{i,h}$ represents wind speed at bus i at state h; H is the number of states, which depends on the resolution requirement. With more wind states, the result will be more accurate but take more computation time too. During the real-time operation, the wind speed evolves stochastically among these states, $v_i(t) \in v_i$. The stochastic process of wind speed can be modeled as a Markov process. The tendency of the transition among these states is modeled as the state transition rate. According to the Markov model, the likelihood of the wind speed at each state h is derived as [13]:

$$\frac{d\mathrm{Pr}_i^{wd,h}(t)}{dt} = \sum_{h'=1}^{H,h'\neq h} \mathrm{Pr}_i^{w,h'}(t)\lambda_{h',h}^{w} - \mathrm{Pr}_i^{wd,h}(t) \sum_{h'=1}^{H,h'\neq h} \lambda_{h,h'}^{w}, \tag{1}$$

(2)

where $\mathrm{Pr}_i^1|_{t=0} = 0, ..., \mathrm{Pr}_i^{h_0}|_{t=0} = 1, ..., \mathrm{Pr}_i^H|_{t=0} = 0$; $\mathrm{Pr}_i^{w,h}(t)$ is the probability of wind speed being in state h, which is a function of time; $\lambda_{h,h'}^{w}$ is the state transition rate of wind from state h to state h'.

The power output of the turbine is related to both the velocity of wind, as well as state of turbine itself. Availability of the turbine can be modeled by two states, which includes the perfect and fault states. Suppose the turbine is at the normal state when $t = 0$. Then, the likelihood of the turbine is given as [13]:

$$\mathrm{Pr}_{i,l}^{wt,1}(t) = \frac{\mu_{i,l}^{wt}}{\mu_{i,l}^{wt} + \lambda_{i,l}^{wt}} + \frac{\lambda_{i,l}^{wt}}{\mu_{i,l}^{wt} + \lambda_{i,l}^{wt}} e^{-(\mu_{i,l}^{wt}+\lambda_{i,l}^{wt})t} \tag{3}$$

$$\mathrm{Pr}_{i,l}^{wt,2}(t) = \frac{\lambda_{i,l}^{wt}}{\mu_{i,l}^{wt} + \lambda_{i,l}^{wt}} \left(1 - e^{-(\mu_{i,l}^{wt}+\lambda_{i,l}^{wt})t}\right) \tag{4}$$

where $\mathrm{Pr}_{i,l}^{wt,1}(t)$ and $\mathrm{Pr}_{i,l}^{wt,2}(t)$ represent the availability and unavailability of the wind turbine in time t; $\lambda_{i,l}^{wt}$ and $\mu_{i,l}^{wt}$ are state transition rates of wind turbine l, respectively.

Then, the electricity output upper limit is determined by:

$$P_i^{wf} = \sum_{l \in \mathcal{L}_i^{wt}} s_{i,l}^{wt} f_{i,l}^{wt}(v_i(t)) \tag{5}$$

where P_i^{wf} is the electricity generation; $\mathcal{L}_i^{wt}$ is set of wind turbine; $s_{i,l}^{wt}$ is the state of the wind turbine, where $s_{i,l}^{wt} = 1$ means the normal state, and $s_{i,l}^{wt} = 0$ means the failure state; $f_{i,l}^{wt}(\cdot)$ is the function depending on the type of wind turbine.

The operational availability of other components, e.g., generators, gas sources, etc. can be modeled similarly.

III. Operational Risk Mitigation Scheme

A. *Objective function and optimization variables*

During the operation, the wind speed may become lower than expected, and the IPGS components, including gas sources, and generators, may also fail, and turn the IPGS from the perfect functioning state into the contingency. Then, the IPGS may need to be re-dispatched to realize a balanced operation. To deliver that, the load may be curtailed, and the gas composition may also become insecure. Therefore, in our ORMS problem, we aim to minimize both load shedding and gas security violations. C^T is the operating cost, including gas security violation cost, load shedding cost, etc.

$$\begin{aligned} \min C^T = &\sum_{i \in \mathcal{I}} \sum_{l \in \mathcal{L}_i^{tpp}} cst_{i,l}(P_{i,l}^{tpp}) + \sum_{i \in \mathcal{I}} \sum_{l \in \mathcal{L}^s} \mu_{i,l}^s q_{i,l}^s \\ &+ \sum_{i \in \mathcal{I}} \mu^{sc}\phi_i + \mu^g GCV_r q_{i,r}^{ct} + \mu^e P_i^{ct} \end{aligned} \tag{6}$$

where $\mathcal{L}_i^{tpp}$, $\mathcal{L}^{\mathrm{s}}$ are the sets of traditional fossil power plants (TPP), gas sources, respectively; $cst_{i,l}$ is the cost function of TPP l ; $\mu_{i,l}^{\mathrm{s}}$ is the nodal gas price; μ^{sc} is penalty price of gas security violation; μ^e and μ^g are the customer damage functions of electricity and gas, respectively; $P_{i,l}^{tpp}$ is the power generation of TPP l; $q_{i,l}^{s}$ is gas production of the gas source l at bus i; ϕ_i is the gas security violation at bus i; $q_{i,r}^{ct}$ and P_i^{ct} are the load shedding of gas component r and the electricity at bus i, respectively.

B. Gas system constraints with varying hydrogen injections

The gas system includes the following constraints. This model is extended from our previous work [12].

$$GCV^{\mathrm{ng}} q_i^{\mathrm{d,ng}} = \sum_{r\in\mathcal{R}} (q_{i,r}^{\mathrm{d}} + q_{i,r}^{\mathrm{ct}}) GCV_r,\ q_{i,r}^{\mathrm{d}}, q_{i,r}^{\mathrm{ct}} \geq 0 \tag{7}$$

$$q_{i,r}^{\mathrm{d}} / \sum_{r\in\mathcal{R}} q_{i,r}^{\mathrm{d}} = x_{i,r} \tag{8}$$

$$q_{i,l,r}^{\mathrm{s}} = x_{i,l,r}^{\mathrm{s}} q_{i,l}^{\mathrm{s}} \tag{9}$$

$$q_{i,l}^{\mathrm{s,min}} \leq q_{i,l}^{\mathrm{s}} \leq q_{i,l}^{\mathrm{s,max}} \tag{10}$$

$$q_{i,j}^2 = C_{i,j}^2 (p_i^2 - p_j^2) \tag{11}$$

$$C_{i,j}^2 = \frac{\pi^2 D_{i,j}^5}{F_{i,j} R_{i,j} L_{i,j} Z_{i,j} T^{\mathrm{gas}}} \tag{12}$$

$$q_{i,j} = \sum_{r\in\mathcal{R}} q_{i,j,r} \tag{13}$$

$$|q_{i,j}| \leq q_{i,j}^{\mathrm{max}} \tag{14}$$

$$p_i^{\mathrm{min}} \leq p_i \leq p_i^{\mathrm{max}} \tag{15}$$

$$\sum_{l\in\mathcal{L}_i^{\mathrm{s}}} q_{i,l,r}^{\mathrm{s}} - q_{i,r}^{\mathrm{d}} + \sum_{l\in\mathcal{L}_i^{\mathrm{ptg}}} q_{i,l,r}^{\mathrm{ptg}} - \sum_{l\in\mathcal{L}_i^{\mathrm{gpp}}} q_{i,l,r}^{\mathrm{gpp}} - \sum_{j\in\mathcal{J}_i} q_{i,j,r} = 0, \forall r \in \mathcal{R} \tag{16}$$

$$I_{i,r} = \sum_{j\in\mathcal{J}_i} \frac{\gamma_{i,j}-1}{2} q_{i,j,r} + \sum_{l\in\mathcal{L}_i^{\mathrm{s}}} q_{i,l,r}^{\mathrm{s}} + \sum_{l\in\mathcal{L}_i^{\mathrm{ptg}}} q_{i,l,r}^{\mathrm{ptg}} \tag{17}$$

$$x_{i,r} = I_{i,r}/I_i,\ I_i = \sum_{r\in\mathcal{R}} I_{i,r} \tag{18}$$

$$S_i = \sum_{r\in\mathcal{R}} M_r x_{i,r} / M^{\mathrm{air}} \tag{19}$$

where $I_{i,r}$ is the sum of gas component r that flows into the gas bus i, and I_i is the sum of all gas components that flows into the gas bus i; the meanings of other variables and parameters can be found in [12].

C. Electricity network constraints

The electricity network constraints are presented as follows [12]:

$$\sum_{l\in\mathcal{L}_i^{tpp}} P_{i,l}^{tpp} + \sum_{l\in\mathcal{L}_i^{gpp}} P_{i,l}^{gpp} + \sum_{l\in\mathcal{L}_i^{rng}} P_{i,l}^{rng} - \sum_{l\in\mathcal{L}_i^{ptg}} P_{i,l}^{ptg} - P_i^d - \sum_{j\in\mathcal{J}_i} P_{ij} = 0 \tag{20}$$

$$P_{ij} = (\theta_i - \theta_j)/X_{ij} \tag{21}$$

$$|P_{ij}| \leq P_{ij}^{max} \tag{22}$$

$$P_{i,l}^{tpp,min,h} \leq P_{i,l}^{tpp} \leq P_{i,l}^{tpp,max,h} \tag{23}$$

$$P_{i,l}^{gpp,min,h} \leq P_{i,l}^{gpp} \leq P_{i,l}^{gpp,max,h} \tag{24}$$

$$P_{i,l}^{rng,min,h} \leq P_{i,l}^{rng} \leq P_{i,l}^{rng,max,h} \tag{25}$$

where the meanings of other variables and parameters can be found in [12].

D. Coupling components constraints

The coupling components between the power and gas systems include PTGs and GPPs. Their mathematical model is elaborated as follows. (26) - (28) are the constraints for PTGs. (26) describes the energy conversion relationships of the electrolysis and methanation processes in the PTGs. (27)describes the gas production of PTG. (28) describes the electricity consumption limit for PTGs. (29) and (30) are the constraints for GPPs, where (29) describes the energy conversion efficiency, and (30) enforces the composition of consumed gas should be equal to the gas composition at the specific bus.

$$P_{i,l}^{\mathrm{ptg}} \eta_{i,l}^{\mathrm{e}} = q_{i,l}^{\mathrm{hy}} GCV^{\mathrm{hy}} + q_{i,l}^{\mathrm{me}} GCV^{\mathrm{me}} / \eta_{i,l}^{\mathrm{me}} \tag{26}$$

$$q_{i,l}^{\mathrm{ptg}} = \sum_{r\in\mathcal{R}} q_{i,l,r}^{\mathrm{ptg}} = q_{i,l}^{\mathrm{hy}} + q_{i,l}^{\mathrm{me}},\ q_{i,l}^{\mathrm{hy}} \geq 0, q_{i,l}^{\mathrm{me}} \geq 0 \tag{27}$$

$$0 \leq P_{i,l}^{\mathrm{ptg}} \leq P_{i,l}^{\mathrm{ptg,max,h}} \tag{28}$$

$$P_{i,l}^{\mathrm{gpp}} = \eta_{i,l}^{\mathrm{gpp}} \sum_{r\in\mathcal{R}} q_{i,l,r}^{\mathrm{gpp}} GCV_r,\ q_{i,l,r}^{\mathrm{gpp}} \geq 0 \tag{29}$$

$$q_{i,l,r}^{\mathrm{gpp}} / \sum_{r\in\mathcal{R}} q_{i,l,r}^{\mathrm{gpp}} = x_{i,r} \tag{30}$$

where $P_{i,l}^{\mathrm{ptg}}$ is the electricity consumed by PTG l at bus i; $\eta_{i,j}^{\mathrm{e}}$ and $\eta_{i,l}^{\mathrm{me}}$ are the efficiencies of electrolysis and methanation processes, respectively; GCV^{hy} and GCV^{me} are the GCVs of methane and hydrogen, respectively; $q_{i,l}^{\mathrm{hy}}$ and $q_{i,l}^{\mathrm{me}}$ are the hydrogen and methane productions of PTG l at bus i, respectively; $P_{i,l}^{\mathrm{ptg,max,h}}$ is the maximum electricity consumption of the PTG l at bus i in state$h$; $P_{i,l}^{\mathrm{gpp}}$ is the electricity generation of GPP l at bus i; $\eta_{i,l}^{\mathrm{gpp}}$ is the efficiency of the GPP l; $q_{i,l,r}^{\mathrm{gpp}}$ is the gas component r consumed by the GPP l.

IV. Operational Risk Evaluation Procedures

The operational risk of the IPGS is analyzed by using the analytical-based method, which can reduce the CPU time. Procedures are shown as:

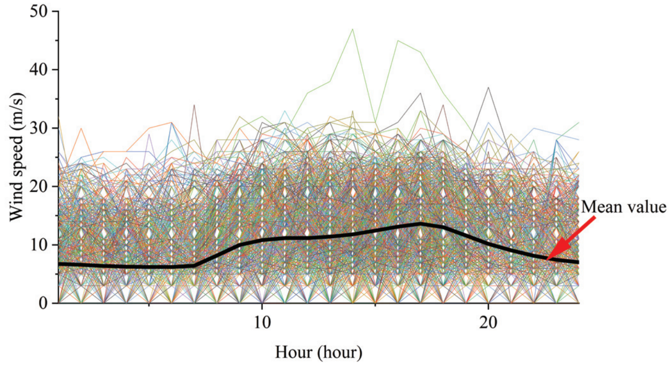

Fig. 1. Wind speed dataset

Step 1: Initialize the IPGS parameters, historical wind speed, and failure/repair rates of other system components.

Step 2: Cluster the wind speed into H states according to the historical data. Calculate the state transition rates according to [14].

Step 3: Initialize states of system components when $t = 0$. Calculate the state probability of components during the operation horizon according to Section II. Combine the component states into the system states, and calculate the probability of each system state.

State 4: For each system state, solve the ORMS problem formulated in Section III. Obtain the load shedding $q_{i,r,s}^{\mathrm{ct}}$, $P_{i,s}^{\mathrm{ct}}$ and the gas security indices, such as Wobbe index $WI_{i,s}$ [15], flame speed factor $FS_{i,s}$ [16], etc.

$$WI_{i,s} = \sum_{r\in R} GCV_r x_{i,r}/\sqrt{S_i} \tag{31}$$

$$FS_{i,s} = \frac{\sum_{r\in R} x_{i,r} fs_r}{AF + 5x_i^{\mathrm{N}} - 18.8x_i^{\mathrm{O}} + 1} \tag{32}$$

where GCV_i is the gross caloric value (GCV) of the gas at bus i; GCV_r is the GCV of the gas component r; fs_r is the burning velocity of gas component r in a stoichiometric air mixture; AF is the air-fuel ratio; x_i^{N} and x_i^{O} are the molar fractions of inert gas component and oxygen at bus i, respectively.

Step 5: if all the system states are iterated, calculate the operational risk indices according to [17]:

$$EWI_{i,t} = \sum_{s\in\mathcal{S}} \mathrm{Pr}_s WI_{i,t,s} \tag{33}$$

$$EFS_{i,t} = \sum_{s\in\mathcal{S}} \mathrm{Pr}_s FS_{i,t,s} \tag{34}$$

$$EDNS_{i,t} = \sum_{s\in\mathcal{S}} \mathrm{Pr}_s P_{i,t,s}^{\mathrm{ct}} \tag{35}$$

$$EGNS_{i,t} = \sum_{s\in\mathcal{S}} \mathrm{Pr}_s q_{i,t,s}^{\mathrm{ct}} \tag{36}$$

where $EWI_{i,t}$, $EFS_{i,t}$, $EDNS_{i,t}$, and $EGNS_{i,t}$ are the expected Wobbe index (EWI), expected flame speed (EFS), EDNS, and EGNS in bus i in time t; $\mathcal{S}$ is the set of system states, and Pr_s is the probability of system state s.

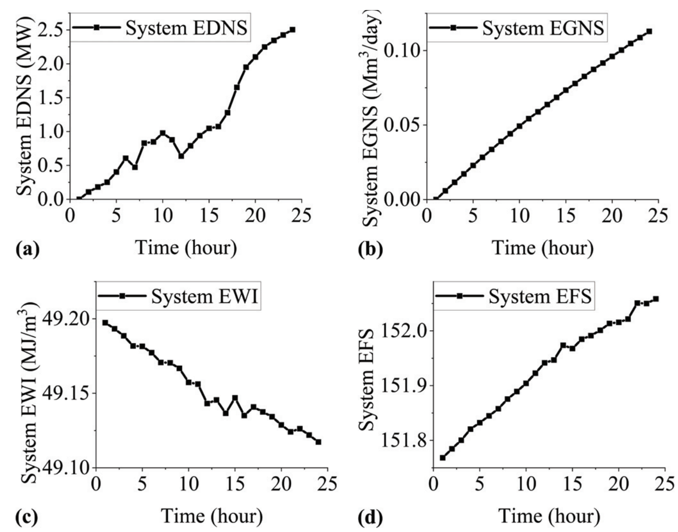

Fig. 2. Operational risk of the IPGS: (a) EDNS; (b) EGNS; (c) EWI; (d) EFS

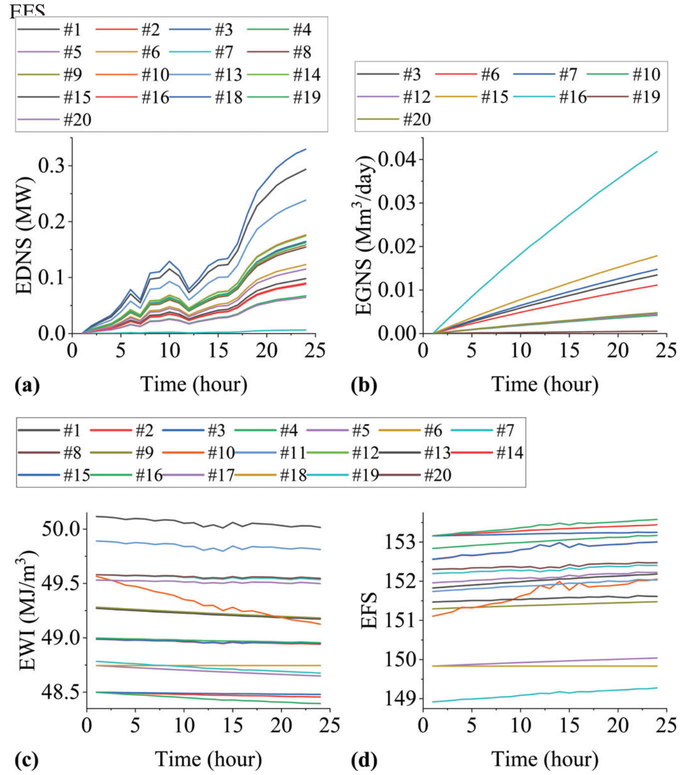

Fig. 3. Nodal operational risks: (a) EDNS; (b) EGNS; (c) EWI; (d) EFS.

V. Case Studies

An IPGS case is applied to varify the proposed GCM and operational risk evaluation techniques. It consists of an IEEE 24 bus RTS [18] and Belgium gas transmission system [19]. They are topologically coupled by GPPs and PTGs. The gas compositions of gas sources are listed in [12]. The wind data is acquired from the National Oceanic and Atmospheric Administration, as shown in Fig. 1. The operational risk evaluation is performed on a desktop.

Whole system's operational risk is demonstrated in Fig. 2. We find that generally, the risks increase with time. For example, the system EDNS and EGNS are 0.1078 MW and 0.0059 Mm^3/day, and their values become 2.505 MW and 0.1129 Mm^3/day, respectively, which are 23.24 and 19.14 times higher. This is because, during the operation, the chances of component failures increase. Therefore, the expected electricity and gas load sheddings increase. The system's EWI decrease, and the EFS increases, both indicating the risk of the gas security violation increase. This is because during the operation, as time goes on, there is a higher chance of gas load shedding. Therefore, the PTG tends to produce more hydrogen to cover the gas supply shortage. As a consequence, the quality of the gas becomes inferior. The hydrogen has a lower Wobbe index and higher flame speed. Thus, if the gas system contains more hydrogen content, the heat value of the gas will be more difficult to meet the standard, and there may be a higher risk of flame hazard.

More specifically, from the nodal point of view, the risk varies in different locations. For example, for EDNS, electricity bus #18 is the highest. This is because renewable energy is located in the electricity bus #18, which is more stochastic. For EGNS, gas bus # 16 is the highest, because it is located in terminal of the pipe route. For EWI, EFS, bus #10 is the most sensitive to time. This is because the gas bus #10 is connected with PTGs, the hydrogen production of which has the most impact on gas bus #10.

VI. Conclusions

This paper proposes an operational risk evaluation approach for IPGS considering varying hydrogen concentrations with high penetration of wind. A multi-state operational availability model of wind generation is developed. Then, an operational risk mitigation scheme is devised to minimize both load shedding and gas security violation. An analytical risk evaluation method, with newly developed risk indices, is used for better computation efficiency.

From the numerical studies, we find the system risk increase with time. Due to the hydrogen injection, the EWI decreases, and the EFS increase. Moreover, different buses present different sensitivities to hydrogen injections. The method and numerical results of this paper can assist the energy company to regulate risks of IPGS with hydrogen injections under high penetration of renewable energies.

References

[1] Department for Business Energy Industrial Strategy, "Energy white paper: Powering our net zero future," 2020.

[2] M. Abeysekera, J. Wu, N. Jenkins, and M. Rees, "Steady state analysis of gas networks with distributed injection of alternative gas," *Applied Energy*, vol. 164, pp. 991–1002, Feb. 2016.

[3] I. Saedi, S. Mhanna, and P. Mancarella, "Integrated electricity and gas system modelling with hydrogen injections and gas composition tracking," *Applied Energy*, vol. 303, p. 117598, 2021.

[4] M. Ban, J. Yu, M. Shahidehpour, and Y. Yao, "Integration of power-to-hydrogen in day-ahead security-constrained unit commitment with high wind penetration," *Journal of Modern Power Systems and Clean Energy*, vol. 5, no. 3, pp. 337–349, 2017.

[5] J. Li, J. Lin, Y. Song, X. Xing, and C. Fu, "Operation optimization of power to hydrogen and heat (p2hh) in adn coordinated with the district heating network," *IEEE Transactions on Sustainable Energy*, vol. 10, no. 4, pp. 1672–1683, 2018.

[6] S. Fang, S. Zhang, T. Zhao, and R. Liao, "Optimal power-hydrogen networked flow scheduling for residential carpark with convex approximation," *IEEE Transactions on Industry Applications*, vol. 58, no. 2, pp. 2751–2759, 2021.

[7] J. Naughton, S. Riaz, M. Cantoni, X.-P. Zhang, and P. Mancarella, "Comprehensive optimization-based techno-economic assessment of hybrid renewable electricity-hydrogen virtual power plants," *Journal of Modern Power Systems and Clean Energy*, 2022.

[8] G. Sun, G. Li, P. Li, S. Xia, Z. Zhu, and M. Shahidehpour, "Coordinated operation of hydrogen-integrated urban transportation and power distribution networks considering fuel cell electric vehicles," *IEEE Transactions on Industry Applications*, vol. 58, no. 2, pp. 2652–2665, 2021.

[9] P. Zhao, C. Gu, Z. Hu, D. Xie, I. Hernando-Gil, and Y. Shen, "Distributionally robust hydrogen optimization with ensured security and multi-energy couplings," *IEEE Transactions on Power Systems*, vol. 36, no. 1, pp. 504–513, 2020.

[10] P. Zhao, X. Lu, Z. Cao, C. Gu, Q. Ai, H. Liu, Y. Bian, and S. Li, "Volt-var-pressure optimization of integrated energy systems with hydrogen injection," *IEEE Transactions on Power Systems*, vol. 36, no. 3, pp. 2403–2415, 2020.

[11] A. De Corato, I. Saedi, S. Riaz, and P. Mancarella, "Aggregated flexibility from multiple power-to-gas units in integrated electricity-gas-hydrogen distribution systems," *Electric Power Systems Research*, vol. 212, p. 108409, 2022.

[12] S. Wang, J. Zhai, and H. Hui, "Optimal energy flow in integrated electricity and gas systems with injection of alternative gas," *IEEE Transactions on Sustainable Energy*, (early access) 2023.

[13] Y. Ding, C. Singh, L. Goel, J. Østergaard, and P. Wang, "Short-term and medium-term reliability evaluation for power systems with high penetration of wind power," *IEEE Transactions on Sustainable Energy*, vol. 5, no. 3, pp. 896–906, 2014.

[14] H. Jia, Y. Ding, Y. Song, C. Singh, and M. Li, "Operating reliability evaluation of power systems considering flexible reserve provider in demand side," *IEEE Transactions on Smart Grid*, vol. 10, no. 3, pp. 3452–3464, 2018.

[15] J. Klimstra, "Interchangeability of gaseous fuels—the importance of the wobbe-index," *SAE transactions*, pp. 962–972, 1986.

[16] C. K. Wu and C. K. Law, "On the determination of laminar flame speeds from stretched flames," in *Symposium (International) on Combustion*, vol. 20, no. 1. Elsevier, 1985, pp. 1941–1949.

[17] M. Wang, H. Gooi, and S. Chen, "Optimising probabilistic spinning reserve using an analytical expected-energy-not-supplied formulation," *IET generation, transmission & distribution*, vol. 5, no. 7, pp. 772–780, 2011.

[18] C. Grigg, P. Wong, P. Albrecht, R. Allan, M. Bhavaraju, R. Billinton, Q. Chen, C. Fong, S. Haddad, S. Kuruganty *et al.*, "The IEEE reliability test system-1996. A report prepared by the reliability test system task force of the application of probability methods subcommittee," *IEEE Transactions on Power Systems*, vol. 14, no. 3, pp. 1010–1020, Aug. 1999.

[19] D. De Wolf and Y. Smeers, "The gas transmission problem solved by an extension of the simplex algorithm," *Management Science*, vol. 46, no. 11, pp. 1454–1465, Nov. 2000.